ARTICLE

Puerarin ameliorated pressure overload-induced cardiac hypertrophy in ovariectomized rats through activation of the PPARα/PGC-1 pathway

Ning Hou[1,2], Yin Huang[1,3], Shao-ai Cai[1], Wen-chang Yuan[2], Li-rong Li[1,2], Xia-wen Liu[1,2], Gan-jian Zhao[1], Xiao-xia Qiu[2], Ai-qun Li[4], Chuan-fang Cheng[1], Shi-ming Liu[1], Xiao-hui Chen[1], Dao-feng Cai[2], Jing-xuan Xie[3], Min-sheng Chen[5] and Cheng-feng Luo[1]

Estrogen deficiency induces cardiac dysfunction and increases the risk of cardiovascular disease in postmenopausal women and in those who underwent bilateral oophorectomy. Previous evidence suggests that puerarin, a phytoestrogen, exerts beneficial effects on cardiac function in patients with cardiac hypertrophy. In this study, we investigated whether puerarin could prevent cardiac hypertrophy and remodeling in ovariectomized, aortic-banded rats. Female SD rats subjected to bilateral ovariectomy (OVX) plus abdominal aortic constriction (AAC). The rats were treated with puerarin (50 mg·kg^{-1}·d^{-1}, ip) for 8 weeks. Then echocardiography was assessed, and the rats were sacrificed, their heart tissues were extracted and allocated for further experiments. We showed that puerarin administration significantly attenuated cardiac hypertrophy and remodeling in AAC-treated OVX rats, which could be attributed to activation of PPARα/PPARγ coactivator-1 (PGC-1) pathway. Puerarin administration significantly increased the expression of estrogen-related receptor α, nuclear respiratory factor 1, and mitochondrial transcription factor A in hearts. Moreover, puerarin administration regulated the expression of metabolic genes in AAC-treated OVX rats. Hypertrophic changes could be induced in neonatal rat cardiomyocytes (NRCM) in vitro by treatment with angiotensin II (Ang II, 1 μM), which was attenuated by co-treatemnt with puerarin (100 μM). We further showed that puerarin decreased Ang II-induced accumulation of non-esterified fatty acids (NEFAs) and deletion of ATP, attenuated the Ang II-induced dissipation of the mitochondrial membrane potential, and improved the mitochondrial dysfunction in NRCM. Furthermore, addition of PPARα antagonist GW6471 (10 μM) partially abolished the anti-hypertrophic effects and metabolic effects of puerarin in NRCM. In conclusion, puerarin prevents cardiac hypertrophy in AAC-treated OVX rats through activation of PPARα/PGC-1 pathway and regulation of energy metabolism remodeling. This may provide a new approach to prevent the development of heart failure in postmenopausal women.

Keywords: cardiac hypertrophy; puerarin; ovariectomy; abdominal aortic constriction; PPARα

INTRODUCTION
Epidemiological evidence shows that the incidence of cardiovascular disease is higher in men than in premenopausal women. However, its incidence increases in postmenopausal women or women who have undergone early ovariectomy (OVX) (oophorectomy) [1]. Sex differences in cardiac remodeling have also been observed in aging and pressure-overloaded human hearts. These findings suggest that due to the reduced estrogen levels after menopause or oophorectomy, women lose an important cardiovascular-protective mechanism and are at greater risk of developing cardiac dysfunction [2]. Nevertheless, long-term hormone replacement therapy remains controversial owing to its serious side effects (i.e., higher occurrence of breast cancer [1] and venous thromboembolism [3]). The currently available pharmacological options for the treatment and prevention of cardiac dysfunction and heart failure in postmenopausal or early ovariectomized women are very limited.

Cardiac hypertrophy occurs due to prolonged elevation in hemodynamic workload. In contrast to physiological hypertrophy, cardiac hypertrophy induced by pathological conditions, including hypertension and aortic stenosis, is referred to as pathological hypertrophy. Pathological cardiac hypertrophy results in ventricular remodeling and interstitial fibrosis accompanied by systolic and diastolic dysfunction [4, 5]. Sustained pathological hypertrophy increases the occurrence of arrhythmia, heart failure, and sudden death [6].

Imbalance in energy substrate utilization plays an important role in the development of cardiac hypertrophy. In the normal

[1]Guangzhou Institute of Cardiovascular Disease, Guangdong Key Laboratory of Vascular Diseases, State Key Laboratory of Respiratory Disease, the Second Affiliated Hospital, Guangzhou Medical University, Guangzhou 510260, China; [2]Key Laboratory of Molecular Target and Clinical Pharmacology, School of Pharmaceutical Sciences and the Fifth Affiliated Hospital, Guangzhou Medical University, Guangzhou 511436, China; [3]Xiangtan Central Hospital, Xiangtan 411100, China; [4]Nanfang College of SUN YAT-SEN University, Guangzhou 510970, China and [5]Guangdong Provincial Biomedical Engineering Technology Research Center for Cardiovascular Disease, Sino-Japanese Cooperation Platform for Translational Research in Heart Failure, Zhujiang Hospital, Southern Medical University, Guangzhou 510280, China
Correspondence: Cheng-feng Luo (rocenphone@gzhmu.edu.cn) or Min-sheng Chen (gzminsheng@vip.163.com)
These authors contributed equally: Ning Hou, Yin Huang, Shao-ai Cai, Wen-chang Yuan

Puerarin prevents cardiac hypertrophy via PPARα in OVX rats
N Hou et al.

56

adult mammalian heart, fatty acids serve as the chief metabolic substrate for the generation of adenosine triphosphate (ATP). However, in the hypertrophic heart, energy substrate utilization switches from fatty acids to carbohydrates, characterized by a decrease in fatty acid oxidation and an increase in glucose utilization [5, 7]. This metabolic profile increases the efficiency of oxygen utilization [8] and provides sufficient fuel for oxidative metabolism [9]. Nonetheless, alteration in the metabolic profile may influence the ability of the heart to cope with metabolic stress, such as myocardial ischemia-reperfusion [5]. Moreover, the reduced utilization of fatty acids may lead to lipid toxicity in the heart [10]. Therefore, it is important to maintain metabolic flexibility and balance of substrate utilization in the heart, as this will improve the overall capacity for ATP generation [9] and cardiac function.

Peroxisome proliferator-activated receptor α (PPARα) has been identified as a key regulator of the metabolic substrate switch in hypertrophic hearts [7, 11, 12]. It has been reported that the expression of PPARα and PPARα-regulated genes decreases in hypertrophied hearts. Notably, the use of a PPARα agonist reverses the downregulation of PPARα-regulated genes and restores fatty acid utilization [12]. PPARγ coactivator-1 (PGC-1) was originally described as a coactivator of PPARγ. PGC-1α and PGC-1β are enriched in tissues with high oxidative capacity, such as the heart. They exert biological effects by directly binding to and enhancing the transcriptional activity of nuclear receptors, including PPARα. PGC-1α and PGC-1β regulate the expression of numerous genes involved in mitochondrial energy metabolism, such as in fatty acid oxidation, oxidative phosphorylation, and ATP synthesis [13]. Accordingly, the PPARα/PGC-1 pathway plays a key role in regulating myocardial bioenergetics, and it is a plausible therapeutic target. However, the role of a defective PPARα/PGC-1 pathway in mediating pathological cardiac hypertrophy in postmenopausal women remains unclear.

Puerarin (7,4′-dihydroxyisoflavone-8β-glucopyranoside) is a major active ingredient in the Chinese medicine *Pueraria radix*. It is extracted from the kudzu root (*Puerarialobata* (Wild) Howe). The pharmacological benefits of puerarin include improvement of microcirculation, scavenging of oxygen free radicals, and amelioration of insulin resistance [14], which make it a potential therapeutic agent against hypertension [15], cerebral ischemia [16], myocardial ischemia [17], diabetes mellitus [18], and arteriosclerosis [19]. It has been reported that puerarin retards the progression of cardiac hypertrophy in mice through the blockade of the phosphoinositide 3-kinase/Akt and c-Jun N-terminal kinase signaling pathways [20]. Other studies suggested that puerarin may exert antihypertrophic efficacy by blocking other hypertrophy-related signaling pathways [21], inhibiting oxidative stress [22, 23], activating autophagy [24], and enhancing the expression of miR-15b and miR-195 [25]. We previously reported that activation of the transcription factor nuclear factor erythroid 2-related factor 2 plays a key role in the prevention of cardiac hypertrophy by puerarin in rats [26]. Improvement or normalization of the myocardial energy metabolic profiles or metabolic flexibility is critical to prevent or retard the transition from cardiac hypertrophy to heart failure. In the present study, we investigated the pharmacological benefits of puerarin on cardiac energy metabolism in a bilateral OVX with pressure-overload rat model and angiotensin II-treated (Ang II-treated) neonatal rat cardiomyocytes (NRCMs). We also investigated whether the PPARα/PGC-1 pathway mediated the antihypertrophic effect of puerarin.

MATERIALS AND METHODS
Materials
Injectable puerarin was purchased from Zhejiang Zhenyuan Pharmaceutical Co., Ltd. (Shaoxing, China). Puerarin, fenofibrate,

GW6471, and Ang II were purchased from Sigma-Aldrich (St. Louis, MO, USA). The Pierce BCA Protein Assay Kit and Pierce ECL Western Blotting Substrate were purchased from Thermo Fisher Scientific (Rockford, IL, USA). RNAiso Plus, PrimeScript RT reagent Kit with gDNA Eraser (Perfect Real Time), and SYBR Premix Ex Taq II (Tli RNase H Plus) were purchased from Takara Bio Inc. (Shiga, Japan). The ATP and JC-1 assay kits were purchased from the Beyotime Institute of Biotechnology (Haimen, China). Oligomycin, carbonylcyanide p-trifluoromethoxyphenylhydrazone (FCCP), and rotenone/antimycin A were purchased from Seahorse Bioscience (Seahorse Bioscience, Billerica, MA, USA) as components of the XF Cell Mito Stress Test Kit. The non-esterified Free Fatty Acid Assay Kit was purchased from Nanjing Jiancheng Bioengineering Institute (Nanjing, China).

Animal model
Female pathogen-free Sprague–Dawley rats (weight: 150–180 g) were purchased from Guangdong Medical Laboratory Animal Center (Guangzhou, China). The animal experiments were conducted following the Guide for the Care and Use of Laboratory Animals published by the US National Institutes of Health (Bethesda, MD, USA). The animal use and care protocol was reviewed and approved by the Ethics Committee of Guangzhou Medical University (Guangzhou, China). The rats were housed in an environmentally controlled room (temperature: $25 \pm 2\,°C$; humidity: $60\% \pm 5\%$; 12-h dark/light cycle) with ad libitum access to regular chow diet for 1 week prior to the experiments.

Animal experimental design and treatment protocol
Bilateral OVX was performed in rats anesthetized with pentobarbital (45 mg·kg^{-1}, intraperitoneal injection). A sham operation was performed by exposing the ovaries without isolation. Cardiac hypertrophy was induced by abdominal aortic constriction (AAC) [26]. Briefly, the rats were anesthetized, the abdominal aorta was exposed under sterile conditions through a midline abdominal incision, and a blunted 18-gauge needle was placed along the abdominal aorta. A ligature (7-0 silk) was snugly tied around both the abdominal aorta and needle above the renal arteries. The needle was subsequently removed, leaving the internal diameter of the aorta approximately equal to that of the needle. The operation was performed in sham rats, and an untied ligature was placed at the same location. Upon completion of the surgery, the rats were injected with buprenorphine and placed on a warming pad until they recovered from the anesthesia. The female Sprague–Dawley rats were randomly assigned to five groups: (1) sham group; (2) ovariectomy plus abdominal aortic constriction (OVX + AAC); (3) ovariectomy plus abdominal aortic constriction with injection of puerarin (Pue; intraperitoneal injection, 50 mg·kg^{-1} body weight [BW]) daily (OVX + AAC + Pue); (4) ovariectomy plus abdominal aortic constriction with injection of 17-β estradiol (E2; subcutaneous injection, 40 μg·kg^{-1} BW) daily (OVX + AAC + E2); and (5) ovariectomy plus abdominal aortic constriction with administration of fenofibrate (Fen; gavage 80 mg·kg^{-1} BW) (OVX + AAC + Fen). Following 8 weeks of drug administration, echocardiography assessments were performed, the rats were sacrificed, and their heart tissues were extracted and allocated for further experiments.

Echocardiography
Prior to transthoracic echocardiography, the rats were preanesthetized in an induction chamber. The rats were placed in the supine position on a heated pad, and anesthesia was maintained via a face mask through continuous isoflurane ventilation on a mixture of room air and oxygen. Echocardiograms of the left ventricle were obtained using a 250-MHz ultrasound transducer (Vevo 2100; Visual Sonics) [26]. M-mode recordings of the left ventricle were obtained in the parasternal short axis view at the level of the LV papillary muscles. Five consecutive cardiac cycles were measured;

Puerarin prevents cardiac hypertrophy via PPARα in OVX rats
N Hou et al.

57
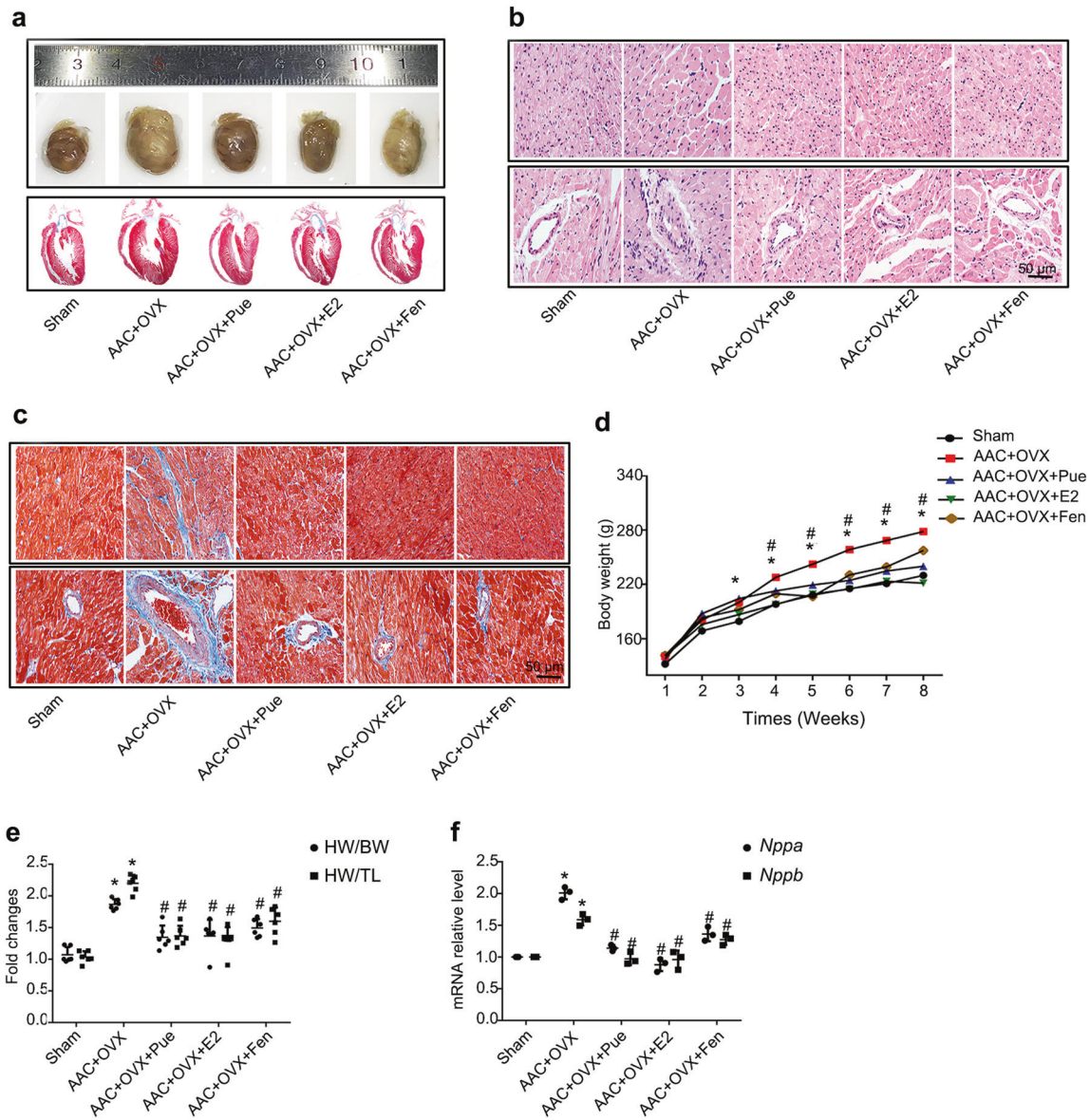
Fig. 1 Puerarin attenuates ovariectomy (OVX) and abdominal aortic constriction (AAC)-induced cardiac hypertrophy. **a** Gross hearts (upper); hematoxylin and eosin (H&E) staining of longitudinal sections of rat hearts (lower). **b** H&E staining of sham and OVX + AAC hearts after 8 weeks of treatment with puerarin. Cross-section of the myocardium (upper). Perivascular cardiomyocytes (lower). Images are representative of three independent staining experiments. **c** Representative images of Masson's trichrome staining for interstitial fibrosis of the myocardium (upper) and perivascular fibrosis (lower) from three staining experiments. **d** Dynamics of body weight. **e** Heart weight/body weight (HW/BW) ratio and heart weight/tibial length (HW/TL) ratio, $n = 6$–8 rats per group. **f** Reverse transcription-polymerase chain reaction analysis of natriuretic peptide A (*Nppa*) and natriuretic peptide B (*Nppb*). Data are representative of three independent experiments. OVX, ovariectomy; AAC, abdominal aortic constriction group; OVX + AAC + Pue, puerarin injected-OVX + AAC group; OVX + AAC + E2, E2 injected-OVX + AAC group; OVX + AAC + Fen, fenofibrate injected-OVX + AAC group. Data are presented as the mean ± SD. Statistical significance was determined using one-way ANOVA coupled with Tukey's multiple comparison post hoc test. *$P < 0.05$ vs. sham group; #$P < 0.05$ vs. OVX + AAC group

the mean value of these cycles was calculated. Measurements of the LV internal dimensions in diastole (LVIDd) and systole (LVIDs), the LV anterior wall in diastole (LVAWd) and systole (LVAWs), and LV posterior wall thickness in diastole (LVPWd) and systole (LVPWs) were performed. These measurements were subsequently used to calculate the LV ejection fraction (LVEF) and fraction shortening (LVFS).

BW and organ weight
The BW of each rat was measured after 2, 4, 6, and 8 weeks of treatment. Following euthanasia through cervical dislocation under anesthesia, the hearts and tibias of rats were immediately harvested and measured. The heart weight (HW)-to-BW ratio and HW-to-tibia length (TL) ratio were used to estimate the degree of cardiac hypertrophy.

Hematoxylin and eosin and Masson's trichrome staining
The hearts were removed and briefly perfused with 10% potassium chloride to arrest the heart in diastole. The hearts were subsequently soaked in 10% formalin and embedded in paraffin. The slides were then dyed with hematoxylin and eosin or Masson's trichrome as previously described [27]. Images were

Puerarin prevents cardiac hypertrophy via PPARα in OVX rats
N Hou et al.

58
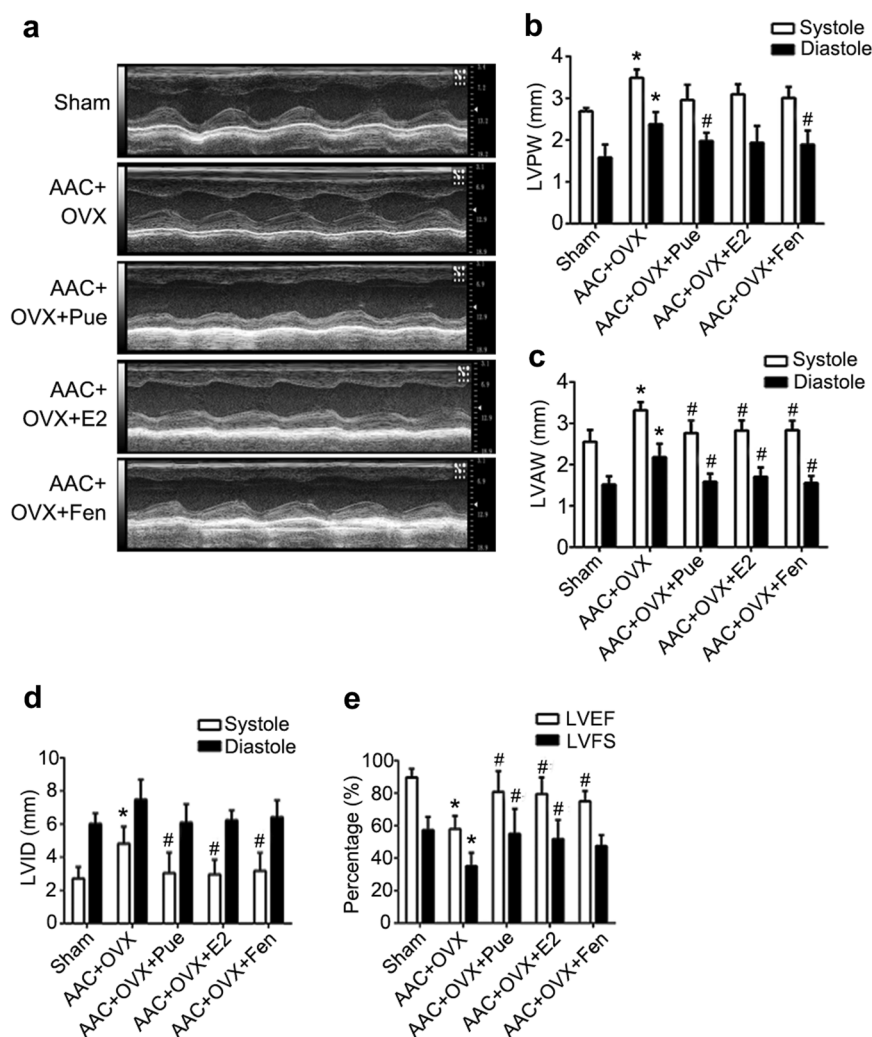
Fig. 2 Puerarin protects against OVX plus AAC-induced cardiac hypertrophy, as indicated by echocardiographic examinations. **a** Representative M-mode images of the indicated groups. **b–d** Parameters of cardiac structure. LVPW left ventricular posterior wall diameter, LVAW left ventricular anterior wall diameter, LVID left ventricular internal dimension. E: Left ventricular function changes in ejection fraction (LVEF) and fractional shortening (LVFS). OVX ovariectomy, AAC abdominal aortic constriction group; OVX + AAC + Pue, puerarin injected-OVX + AAC group; OVX + AAC + E2, E2 injected-OVX + AAC group; OVX + AAC + Fen, fenofibrate injected-OVX + AAC group. Data are presented as the mean ± SD. Statistical significance was determined using one-way ANOVA coupled with Tukey's multiple comparison post hoc test. $^*P < 0.05$ vs. sham group; $^#P < 0.05$ vs. OVX + AAC group, $n = 6$–8 rats per group

visualized and captured using a microscope (Eclipse TS100; Nikon, Tokyo, Japan).

Isolation, culture, and treatment of neonatal rat cardiomyocytes (NRCMs)
NRCMs were isolated from the hearts of 1–3-day-old Sprague–Dawley rats by collagenase digestion and cultured as previously reported [23]. Cultured cardiomyocytes were treated with vehicle alone, Ang II (1 μM) alone, Ang II (1 μM)/puerarin (200 μM), Ang II (1 μM)/E2 (10 nM), Ang II (1 μM)/fenofibrate (25 μM), or Ang II (1 μM)/puerarin (200 μM)/GW6471 (10 μM) for 48 h before the cells were harvested for analysis.

Measurement of cell surface area
The cardiomyocyte surface area was measured as previously reported [23, 28]. Briefly, the treated cardiomyocytes were fixed with 4% paraformaldehyde at room temperature for 10 min and washed with phosphate-buffered saline containing 1% Triton X-100 for 20 min. The slides were blocked with 10% normal goat serum for 1 h and incubated with mouse anti-α-actinin (sarcomeric) antibody at 4 °C overnight. After incubation with Dylight

549-conjugated goat anti-mouse secondary antibody (Abcam, Cambridge, MA, USA) at room temperature for 45 min, cell nuclei were stained with 4′,6-diamidino-2-phenylindole (DAPI; Sigma–Aldrich). The slides were mounted using mounting medium. The surface area of cardiomyocytes was analyzed with NIH ImageJ software (http://rsb.info.nih.gov/ij/). A total of 100 cells from randomly selected fields in five wells were examined for each group.

RNA extraction, cDNA synthesis, and quantitative reverse transcription-polymerase chain reaction (qRT-PCR)
The RNAiso Plus reagent (Takara Bio Inc.) and PrimeScript RT reagent Kit with gDNA Eraser (Takara Bio Inc.) were used to isolate total RNA from frozen tissues or treated cells and to synthesize cDNA, respectively, according to the instructions provided by the manufacturer. Real-time PCR was used to quantify specific mRNA expression using the ABI Prism 7500 System (Applied Biosystems, Foster City, CA, USA). The relative gene expression method (ΔΔ cycle threshold) was used to analyze the real-time PCR data. The sequences of the primer pairs for each gene are shown in Table S1.

Puerarin prevents cardiac hypertrophy via PPARα in OVX rats
N Hou et al.

59

Western blotting analysis

In brief, whole-protein lysates from left ventricular tissues and treated NRCMs were separated by 8%–12% sodium dodecyl sulfate–polyacrylamide gel electrophoresis. Proteins were transferred to polyvinylidene difluoride membranes. The membranes

were incubated overnight at 4 °C with the primary antibodies shown in Table S2. After washing, membranes were incubated with secondary anti-mouse (1:5000; Zhongshan Inc., Beijing, China) or anti-rabbit (1:5000; Zhongshan Inc.) immunoglobulin antibodies conjugated to peroxidase. After thorough washing with Tris-buffered saline with 0.1% Tween-20, immunocomplexes were detected using SuperSignal™ West Pico Chemiluminescent Substrate (Thermo Fisher Scientific, Rockford, IL, USA). Signals on the immunoblot were quantified using Quantity One software (Bio-Rad Laboratories, Inc. Berkeley, CA, USA).

Measurement of mitochondrial membrane potential

The JC-1 assay kit (Beyotime) was employed to measure the mitochondrial membrane potential ($\Delta\Psi m$) of NRCMs according to the instructions provided by the manufacturer. Briefly, after treatment in six-well plates, the cells were washed with phosphate-buffered saline, incubated with the fluorescent probe JC-1 (5,5′,6,6′-tetrachloro-1,1′,3,3′-tetraethylbenzimidazolyl carbocyanine iodide; 2.5 µg·mL^{-1}) for 30 min at 37 °C in the dark, and rinsed twice with incubation buffer. Stained cells were visualized using a Nikon A1 confocal microscope (Nikon Instech Co., Ltd., Tokyo, Japan). Depolarized $\Delta\Psi m$ resulted in a decrease in red fluorescence and an increase in green fluorescence. The ratio of red and green fluorescence intensities was calculated using NIH ImageJ software.

Assessment of mitochondrial function

Mitochondrial function was assessed using the Seahorse XF24 Analyzer (Seahorse Bioscience) by real-time measurement of the cellular oxygen consumption rate (OCR). Briefly, cardiomyocytes were seeded in XF24 cell culture microplates (Seahorse Bioscience) at 1×10^5 cells per well in complete medium. After treatment for 48 h with different drugs, the cardiomyocytes were cultured with unbuffered seahorse assay medium (Seahorse Bioscience) and equilibrated for 1 h at 37 °C in a CO$_2$-free incubator. Subsequently, the cell culture microplate was inserted into the instrument. The basal OCR was acquired, followed by consecutive injections of oligomycin (2 µM), carbonylcyanide p-trifluoromethoxyphenylhydrazone (FCCP, 1 µM), and antimycin A/rotenone (0.5/0.5 µM). The OCR was monitored continuously over time.

Detection of ATP content

The levels of ATP were measured using the ATP Assay Kit (Beyotime, China). Left ventricular tissues or treated NRCMs were lysed with 200 µL of cell lysis reagent (Beyotime) and subsequently quantified using the BCA Protein Assay Kit (Thermo Fisher Scientific, Rockford, IL, USA). Luciferase reagent (1 µL) and dilution buffer (100 µL) were added to 50 µL of lysate, and luminescence was analyzed after a 2-s delay with a 10-s integration on a TriStar^2 S LB942 multimode reader (Berthold Technologies GmbH & Co. KG, Bad Wildbad Germany). A standard curve was generated to calculate the ATP content in the samples. Values were normalized to the total protein content in each sample.

Detection of free fatty acid content

The treated cardiomyocytes were disrupted using a manual cell disruptor and quantified with the BCA Protein Assay Kit. The free
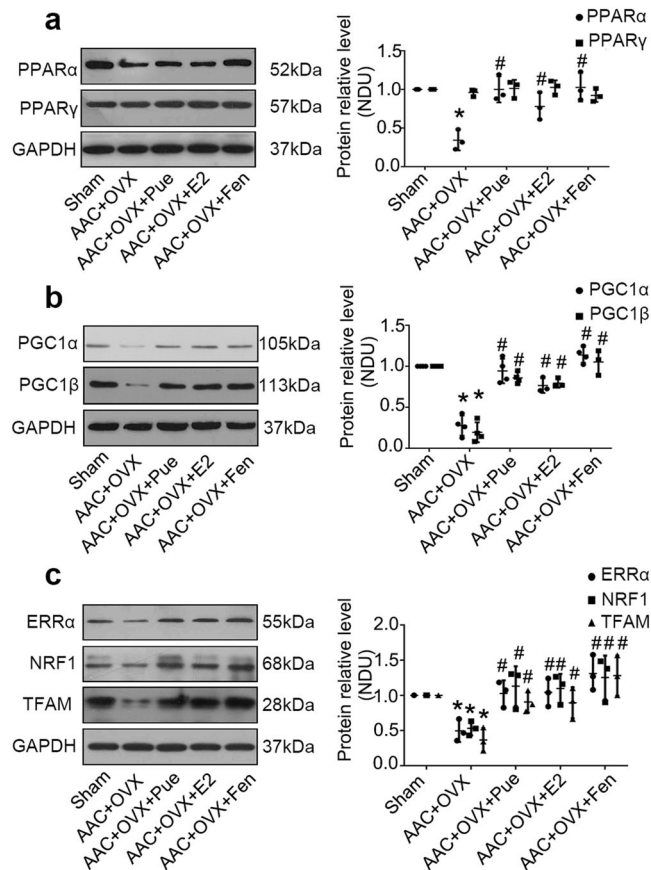
Fig. 3 Puerarin protects against OVX plus AAC-induced cardiac hypertrophy through upregulation of the PPARα/PGC-1 pathway. a Representative Western blots of whole lysates and fold changes in the relative densitometric values of PPARα and PPARγ in hearts obtained from the indicated groups. b Representative Western blots of whole lysates and fold increases in the relative densitometric values of PGC-1α and PGC-1β in hearts. c Representative Western blots of whole lysates and fold increases in the relative densitometric values of estrogen-related receptor alpha (ERRα), nuclear respiratory factor 1 (NRF1) and mitochondrial transcription factor A (TFAM) in hearts. OVX ovariectomy, AAC abdominal aortic constriction group; OVX + AAC + Pue, puerarin injected-OVX + AAC group; OVX + AAC + E2, E2 injected-OVX + AAC group; OVX + AAC + Fen, fenofibrate injected-OVX + AAC group. Data are presented as the mean ± SD. Statistical significance was determined using one-way ANOVA coupled with Tukey's multiple comparison post hoc test. *P < 0.05 vs. sham group; #P < 0.05 vs. OVX + AAC group; representative Western blots and the densitometric analysis from three independent experiments

Table 1. Content of ATP in rats without or with the administration of chemicals 8 weeks after surgery					
	Sham	AAC + OVX	AAC + OVX + Pue	AAC + OVX + E2	AAC + OVX + Fen
ATP (µmol·mg^{-1})	167.15 ± 30.77	72.80 ± 13.92*	200.38 ± 36.41#	170.01 ± 14.36#	126.90 ± 33.38#

Data are presented as the mean ± SD. Statistical significance was determined using one-way ANOVA coupled with Tukey's multiple comparison post hoc test
*P < 0.05 vs. sham group; #P < 0.05 vs. AAC + OVX group; n = 8 rats per group
ATP adenosine triphosphate

Puerarin prevents cardiac hypertrophy via PPARα in OVX rats
N Hou et al.

60
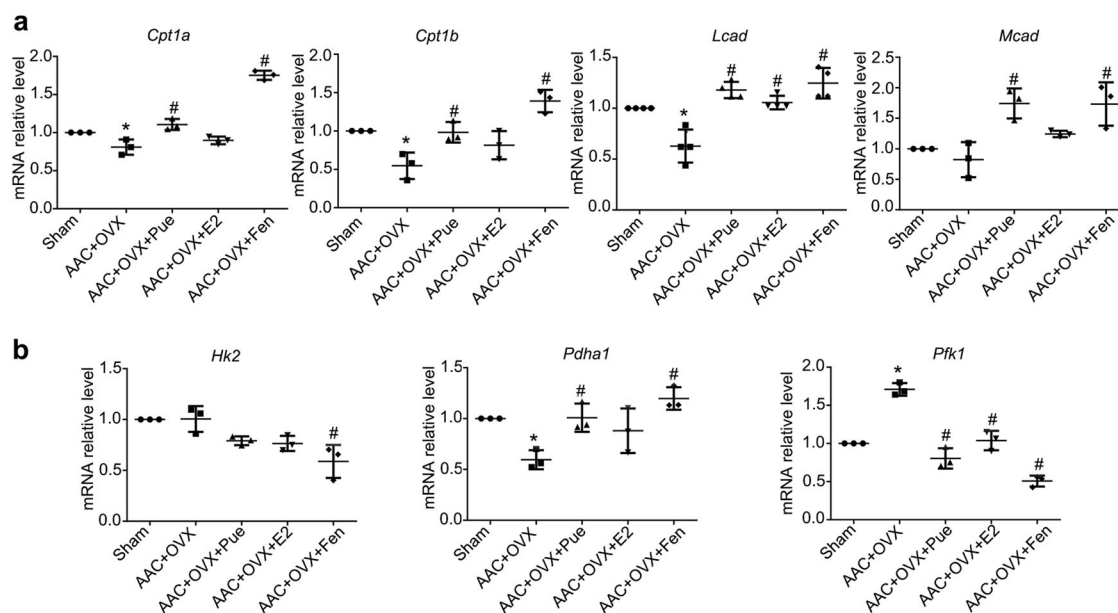
Fig. 4 Puerarin regulates the expression of metabolic genes in cardiac hypertrophy induced by OVX plus AAC surgery. **a** Reverse transcription-polymerase chain reaction analysis for carnitine palmitoyltransferase 1A (*Cpt1a*), carnitine palmitoyltransferase 1B (*Cpt1b*), long-chain acyl-CoA dehydrogenase (*Lcad*), and medium-chain acyl-CoA dehydrogenase (*Mcad*) in hearts obtained from the indicated groups. **b** Reverse transcription-polymerase chain reaction analysis of hexokinase 2 (*Hk2*), pyruvate dehydrogenase E1 component subunit alpha (*Pdha1*), and phosphofructokinase 1 (*Pfk1*) in hearts. OVX ovariectomy, AAC abdominal aortic constriction group; OVX + AAC + Pue, puerarin injected-OVX + AAC group; OVX + AAC + E2, E2 injected-OVX + AAC group; OVX + AAC + Fen, fenofibrate injected-OVX + AAC group. Data are presented as the mean ± SD. Statistical significance was determined using one-way ANOVA coupled with Tukey's multiple comparison post hoc test. $^*P < 0.05$ vs. sham group; $^\#P < 0.05$ vs. OVX + AAC group; data are representative of three independent experiments

fatty acid content was detected using the Non-esterified Free Fatty Acid Assay Kit (Nanjing Jiancheng Bioengineering Institute).

Statistical analysis
Data are presented as means ± standard deviation (SD). Statistical analysis was performed using SPSS 18.0 software (IBM Corporation, Armonk, NY, USA). Statistical differences between the groups were analyzed through one-way analysis of variance, followed by a post hoc Tukey test. A $P < 0.05$ denoted a statistically significant difference.

RESULTS
Puerarin attenuates cardiac hypertrophy in AAC-treated OVX rats
Using a female rat model of OVX plus AAC-induced cardiac hypertrophy, we evaluated whether puerarin would attenuate cardiac hypertrophy and ventricular remodeling at a dose of 50 mg·kg^{-1} per day, as in our previous report [26]. After 8 weeks, the rats subjected to OVX plus AAC surgery showed increased cardiac mass (Fig. 1a), myocyte cross-sectional area (Fig. 1b, c), BW (Fig. 1d), HW/BW ratio, and HW/TL ratio (Fig. 1e) versus the sham group. These findings suggested the presence of cardiac hypertrophy in the OVX + AAC group. The administration of puerarin for 8 weeks significantly attenuated the aforementioned hypertrophic manifestations and BW (Fig. 1a, b, d, e). We further examined the expression of hypertrophic genes. As shown in Fig. 1f, the mRNA expression of natriuretic peptides A and B (*Nppa*, *Nppb*), which were upregulated after OVX plus AAC surgery, was significantly blunted in the rats injected with puerarin. Myocardial fibrosis is a key feature of cardiac remodeling. Therefore, Masson's trichrome staining of cardiac tissue sections was performed to evaluate the severity of myocardial interstitial and perivascular fibrosis in each group. As shown in Fig. 1c, marked interstitial and perivascular fibrosis was observed 8 weeks after OVX plus AAC

surgery; administration of puerarin ameliorated the fibrosis. The protective effect of puerarin on cardiac hypertrophy induced by OVX plus AAC was further evaluated through echocardiography. As shown in Fig. 2, 8 weeks after OVX plus AAC surgery, hypertrophic indicators (i.e., LVPWd, LVPWs, LVAWd, and LVAWs) significantly increased in the OVX + AAC group (Fig. 2a–c) compared with the sham group. Conversely, LVIDs decreased in rats who underwent OVX plus AAC surgery (Fig. 2d). The administration of puerarin resulted in a significant reversal of these hypertrophic indicators (Fig. 2a–d). LVEF and LVFS were also markedly increased in AAC-treated OVX rats (Fig. 2e), and administration of puerarin led to a significant reversal of LVEF and LVFS. The administration of E2 and fenofibrate showed similar potency in inhibiting OVX plus AAC-induced cardiac hypertrophy.

Puerarin protects against cardiac hypertrophy via activation of the PPARα/PGC-1 pathway in AAC-treated OVX rats
PPARα is a ligand-activated transcription factor belonging to the nuclear hormone receptor superfamily and a critical regulator of myocardial metabolism. It has been reported that the occurrence and development of pathological cardiac hypertrophy are associated with the decreased expression and deactivation of PPARα [29]. We evaluated the expression of PPARα, PPARγ, PGC-1α, and PGC-1β by Western blotting in heart tissues obtained from each group to assess whether puerarin would activate the PPARα pathway in AAC-treated OVX rats (Fig. 3). Although the expression of PPARγ protein did not show a significant difference between the sham group and OVX + AAC group, the protein levels of PPARα, PGC-1α, and PGC-1β were significantly decreased in the cardiac tissues of the latter group. Moreover, treatment with puerarin significantly increased the levels of PPARα, PGC-1α, and PGC-1β protein in the rat hearts (Fig. 3a, b). We further measured the protein levels of estrogen-related receptor alpha (ERRα), nuclear respiratory factor 1 (NRF1) and mitochondrial transcription factor

Puerarin prevents cardiac hypertrophy via PPARα in OVX rats
N Hou et al.

61
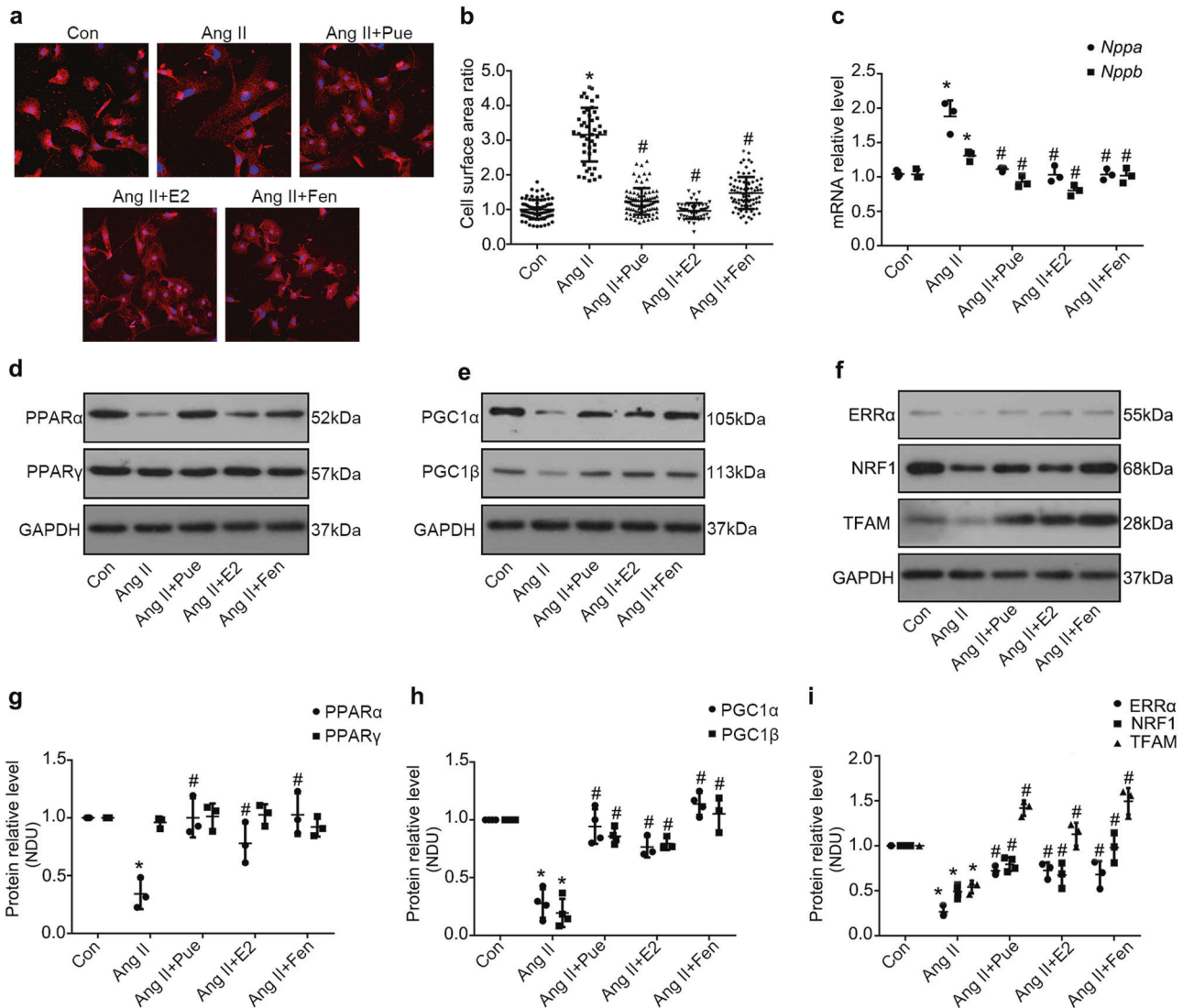
Fig. 5 Puerarin upregulates the PPARα/PGC-1 pathway in Ang II-induced cardiomyocyte hypertrophy. **a, b**: Representative confocal images (**a**) and measurement of surface area (**b**) of cardiomyocytes subjected to different treatments, as indicated; $n = 40$–50 cells per group. **c** Reverse transcription-polymerase chain reaction analysis of atrial natriuretic peptide A (*Nppa*) and natriuretic peptide B (*Nppb*) in NRCMs subjected to the given treatments. Data are representative of three independent experiments. **d, g** Representative Western blots of whole lysates (**d**) and fold increases in the relative densitometric values of PPARα and PPARγ (**g**) in each group. **e** and **h**: Representative Western blots of whole lysates (**e**) and fold increases in the relative densitometric values of PGC-1α and PGC-1β (**h**) in each group. **f, i** Representative Western blots of whole lysates (**f**) and fold increases in the relative densitometric values of estrogen-related receptor alpha (ERRα), nuclear respiratory factor 1 (NRF1), and mitochondrial transcription factor A (TFAM) (**i**) in each group. Data are presented as the mean ± SD. Statistical significance was determined using one-way ANOVA coupled with Tukey's multiple comparison post hoc test. *$P < 0.05$ vs. Con group; #$P < 0.05$ vs. Ang II group; representative Western blots and the densitometric analysis from three or four independent experiments

A (TFAM), which are involved in the regulation of mitochondrial biogenesis and are regulated by the PPARα/PGC-1 pathway. The expression of ERRα, NRF1, and TFAM was decreased in cardiac tissues obtained from rats who underwent OVX plus AAC surgery compared with that reported in the sham group. Puerarin markedly increased these protein levels in OVX + AAC + Pue rats (Fig. 3c). In addition, we examined the contents of ATP in hearts obtained from the different groups. As shown in Table 1, compared with the sham group, the ATP content was significantly lower in the hearts of OVX + AAC rats and higher in the hearts of rats treated with puerarin. We further measured the mitochondrial DNA (mtDNA) content to evaluate mitochondrial biogenesis, which plays a crucial role in preserving metabolic function. As shown in Fig. S1, the AAC + OVX-induced mtDNA content

substantially decreased compared with sham. Treatment with puerarin markedly increased the mtDNA content. Administration of E2 and fenofibrate showed similar potency in improving the PPARα/PGC-1 pathway, ATP content, and mtDNA content.

Puerarin regulates the expression of metabolic genes in AAC-treated OVX rats

Emerging evidence indicates that PPARα and its cardiac-enriched coactivator protein PGC-1 play important roles in the transcriptional control of myocardial energy metabolism. The PPARα-PGC-1 complex controls the expression of genes encoding enzymes involved in cardiac fatty acid and glucose metabolism. We further performed reverse transcription-PCR to examine the mRNA expression of metabolic genes. As shown in Fig. 4, the expression

Puerarin prevents cardiac hypertrophy via PPARα in OVX rats
N Hou et al.

62
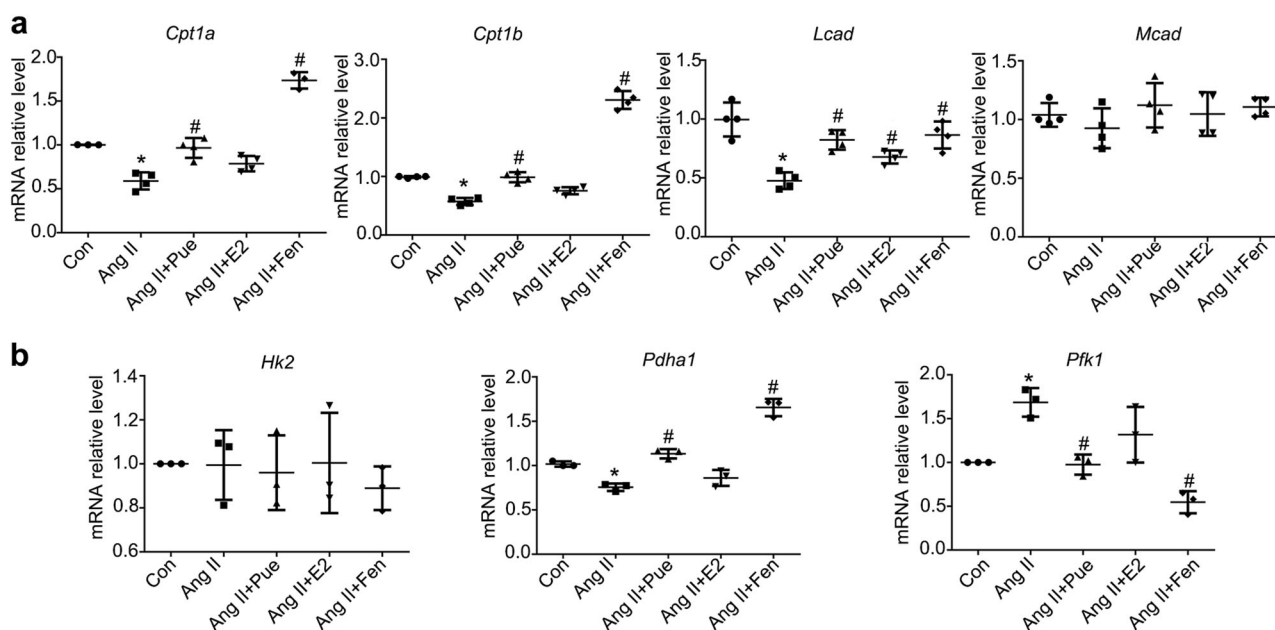
Fig. 6 Puerarin regulates the expression of metabolic genes in Ang II-induced cardiomyocyte hypertrophy. **a** Reverse transcription-polymerase chain reaction analysis of carnitine palmitoyltransferase 1A (*Cpt1a*), carnitine palmitoyltransferase 1B (*Cpt1b*), long-chain acyl-CoA dehydrogenase (*Lcad*), and medium-chain acyl-CoA dehydrogenase (*Mcad*) in the indicated groups. **b** Reverse transcription-polymerase chain reaction analysis of hexokinase 2 (*Hk2*), pyruvate dehydrogenase E1 component subunit alpha (*Pdha1*), and phosphofructokinase 1 (*Pfk1*) in cardiomyocytes. Data are presented as the mean ± SD. Statistical significance was determined using one-way ANOVA coupled with Tukey's multiple comparison post hoc test. $^{*}P < 0.05$ vs. Con group; $^{\#}P < 0.05$ vs. Ang II group; data are representative of three independent experiments

Table 2. Content of ATP and NEFA in Ang II-treated NRCMs without or with the administration of chemicals

	Con	Ang II	Ang II + Pue	Ang II + E2	Ang II + Fen
ATP (µmol·mg^{-1})	197.50 ± 26.10	80.21 ± 11.14*	239.13 ± 87.74$^{\#}$	238.94 ± 44.66$^{\#}$	196.51 ± 12.82$^{\#}$
NEFA (mmol·mg^{-1})	0.23 ± 0.08	0.54 ± 0.13*	0.27 ± 0.10$^{\#}$	0.40 ± 0.08	0.30 ± 0.14

Data are presented as the mean ± SD. Statistical significance was determined using one-way ANOVA coupled with Tukey's multiple comparison post hoc test. $^{*}P < 0.05$ vs. control group; $^{\#}P < 0.05$ vs. Ang II group. Data are representative of six independent experiments
ATP adenosine triphosphate, *NEFA* nonesterified fatty acid, *NRCMs* neonatal rat cardiomyocytes

of glucolipid metabolism-related genes carnitine palmitoyltransferase 1A (*Cpt1a*), carnitine palmitoyltransferase 1B (*Cpt1b*), long-chain acyl-CoA dehydrogenase (*Lcad*), and pyruvate dehydrogenase E1 component subunit alpha (*Pdha1*) was significantly downregulated, whereas that of phosphofructokinase 1 (*Pfk1*) was drastically upregulated in the AAC + OVX group versus the sham group. Conversely, treatment with puerarin markedly increased the mRNA levels of *Cpt1a, Cpt1b, Lcad*, and *Pdha1*, whereas it decreased those of *Pfk1*. The expression of hexokinase 2 (*Hk2*) did not show a significant difference in any of the groups.

Puerarin activates the PPARα/PGC-1 pathway in Ang II-induced cardiomyocyte hypertrophy
Furthermore, we determined whether puerarin could activate the PPARα/PGC-1 pathway to improve cardiac energy metabolism in the pathophysiological process of cardiac hypertrophy. For this purpose, we examined its effects on hypertrophic changes in NRCMs induced by Ang II. Consistent with our previous findings [26], these hypertrophic changes induced by Ang II (1 µM) were attenuated by cotreatment with puerarin (100 µM) (Fig. 5a–c). We further evaluated the protein levels of the PPARα/PGC-1 pathway using Western blotting. As shown in Fig. 5d, e, g, h, reduced levels of PPARα, PGC-1α, and PGC-1β were observed in Ang II-treated cardiomyocytes. Notably, these effects were reversed by treatment

with puerarin. Moreover, Ang II obviously decreased the protein levels of ERRα, NRF1, and TFAM. Consistent with the in vivo data, coincubation with puerarin restored the expression induced by Ang II (Fig. 5f, i). In addition, we evaluated the expression of metabolic genes. Similar to the rats in the OVX + AAC group, treatment with Ang II decreased the mRNA expression of *Cpt1a, Cpt1b, Lcad*, and *Pdha1*, whereas it increased that of *Pfk1*. These effects were blocked by treatment with puerarin (Fig. 6). Administration of E2 and fenofibrate showed similar potency in the reversal of hypertrophic indicators and improvement of the PPARα/PGC-1 pathway.

Puerarin improves the Ang II-induced accumulation of nonesterified fatty acids (NEFAs) and ATP insufficiency
As shown in Table 2, the NEFA content in the Ang II-treated group was significantly higher than that measured in the control group; however, it was lower in the puerarin coincubation group. Conversely, the ATP content was markedly lower in the Ang II-treated group but higher in the puerarin coincubation group than in the control group (Table 2).

Puerarin attenuates the Ang II-induced dissipation of the mitochondrial membrane potential (ΔΨm)
I is well established that maintenance of an intact ΔΨm is critical for cell survival. Thus, the involvement of mitochondria in the

Puerarin prevents cardiac hypertrophy via PPARα in OVX rats
N Hou et al.

63
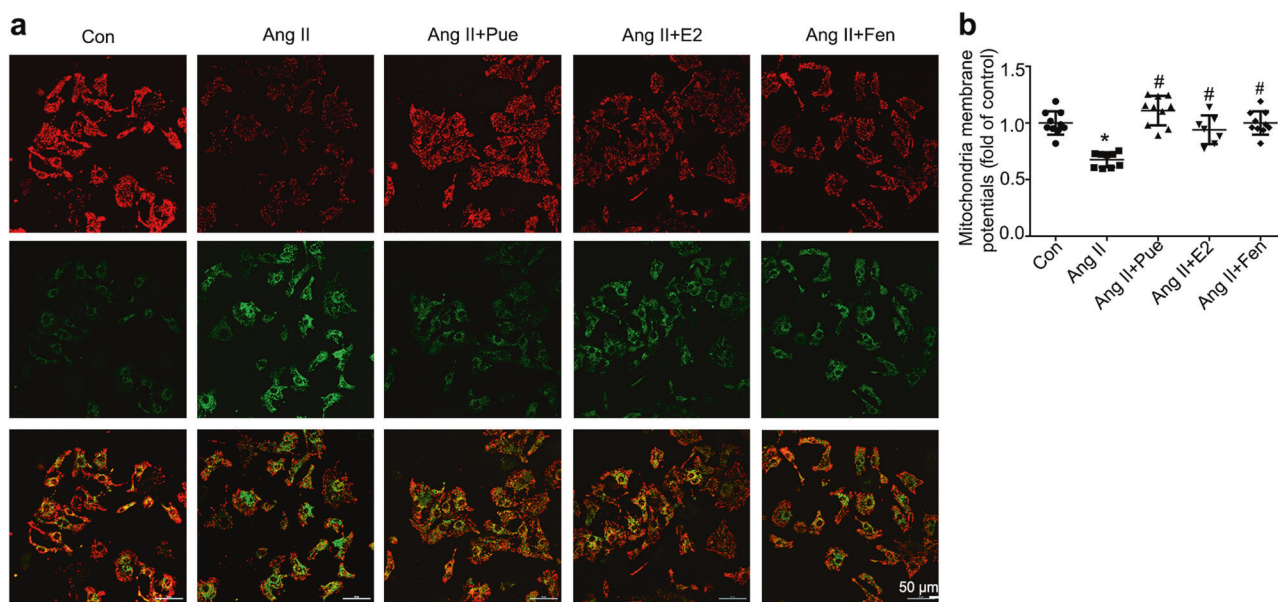
Fig. 7 Puerarin attenuates Ang II-induced dissipation of the mitochondrial membrane potential (ΔΨm) in cardiomyocytes. **a** Representative confocal images of JC-1 staining. Scale bar = 50 μm. **b** Quantitative analysis of JC-1 fluorescence in treated cardiomyocytes. Red fluorescence represents the mitochondrial aggregate form of JC-1, indicating an intact ΔΨm. Green fluorescence represents the monomeric form of JC-1, indicating dissipation of the ΔΨm. Data are presented as the mean ± SD. Statistical significance was determined using one-way ANOVA coupled with Tukey's multiple comparison post hoc test. $^*P < 0.05$ vs. Con group; $^\#P < 0.05$ vs. Ang II group, $n = 10$–12 cells per group

initiation of cardiomyocyte hypertrophy was evaluated though JC-1 staining of treated cardiomyocytes. Under the control conditions, cardiomyocytes were stained with JC-1, simultaneously emitting high-density red fluorescence and low-density green fluorescence (Fig. 7). This aggregated JC-1 within normal mitochondria was dispersed to the monomeric form after treatment with Ang II for 48 h, emitting green fluorescence (Fig. 7). The ratio of JC-1 red/green fluorescence intensity was obviously decreased in the cardiomyocytes treated with Ang II compared with that calculated for the control. Treatment with puerarin reversed the ratio of JC-1 red/green fluorescence intensity and improved the ΔΨm. E2 and fenofibrate showed similar potency in attenuating Ang II-induced dissipation of ΔΨm (Fig. 7).

Puerarin improves the Ang II-induced mitochondrial dysfunction
We also assessed the mitochondrial function in treated cardiomyocytes. The mitochondrial stress test was performed to monitor the cellular OCR in response to oligomycin A, followed by FCCP and rotenone/antimycin A (Rot/ant-A, 0.5/0.5 μM) in real time (Fig. 8a). This test provides information regarding the basal respiration, ATP-linked respiration, proton leak, maximal respiration capacity, and nonmitochondrial respiration of treated cardiomyocytes. As shown in Fig. 8, nonmitochondrial respiration (b), basal respiration (c), ATP turnover (d), maximal respiration capacity (e), and proton leakage (f) were drastically decreased in cardiomyocytes treated with Ang II. The impaired mitochondrial function was partially reversed by treatment with puerarin.

Puerarin protects against Ang II-induced cardiomyocyte hypertrophy through the activation of PPARα
The role of PPARα in the antihypertrophic effect of puerarin was further confirmed using the PPARα antagonist GW6471. NRCMs were treated with Ang II (1 μM) alone, both Ang II (1 μM) and puerarin (100 μM), or Ang II (1 μM), puerarin (100 μM), and

GW6471 (10 μM). After coincubation with GW6471 for 48 h, the antihypertrophic effects of puerarin were attenuated. The puerarin-induced downregulation of hypertrophic indicators, such as cell surface area and hypertrophic genes, was also partially abolished after treatment with GW6471 (Fig. 9a, b). As demonstrated in Fig. 9c, d, GW6471 drastically inhibited the protein expression of PPARα, PGC-1α, PGC-1β, ERRα, NRF1, and TFAM. The expression of puerarin-regulated metabolic genes was abolished after treatment with GW6471 (Fig. 9e). We also evaluated the ΔΨm, ATP content, and NEFA content, which were improved after treatment with puerarin. As with the hypertrophic indicators, coincubation with GW6471 partially abolished the puerarin-induced improvements of ΔΨm (Fig. 9f), ATP content (Table 3), and NEFA content (Table 3).

DISCUSSION
Previous studies have reported that treatment with puerarin prevents cardiac hypertrophy induced by pressure overload [20, 24, 26] or Ang II [22, 25]. Similar results were shown in the present study. Moreover, puerarin upregulated the expression of PPARα, PGC-1α, and PGC-1β, increased the expression of genes related to fatty acid metabolism, decreased the expression of genes related to glucose metabolism, enhanced fatty acid utilization, increased the generation of ATP, and improved mitochondrial function. Furthermore, the PPARα inhibitor GW6471 blocked these puerarin-induced effects.

Although cardiovascular events are rare in premenopausal women, their incidence markedly increases at the age of 45–54 years (i.e., onset of menopause) [1]. Weight gain is frequently observed in perimenopausal women who are not receiving hormone replacement therapy [1]. It is mainly attributed to an increase in abdominal subcutaneous and visceral fat. The accumulation of abdominal fat and increased body mass index tend to reduce insulin sensitivity and increase systolic blood pressure [1, 30]. However, long-term hormone replacement

Puerarin prevents cardiac hypertrophy via PPARα in OVX rats
N Hou et al.

64
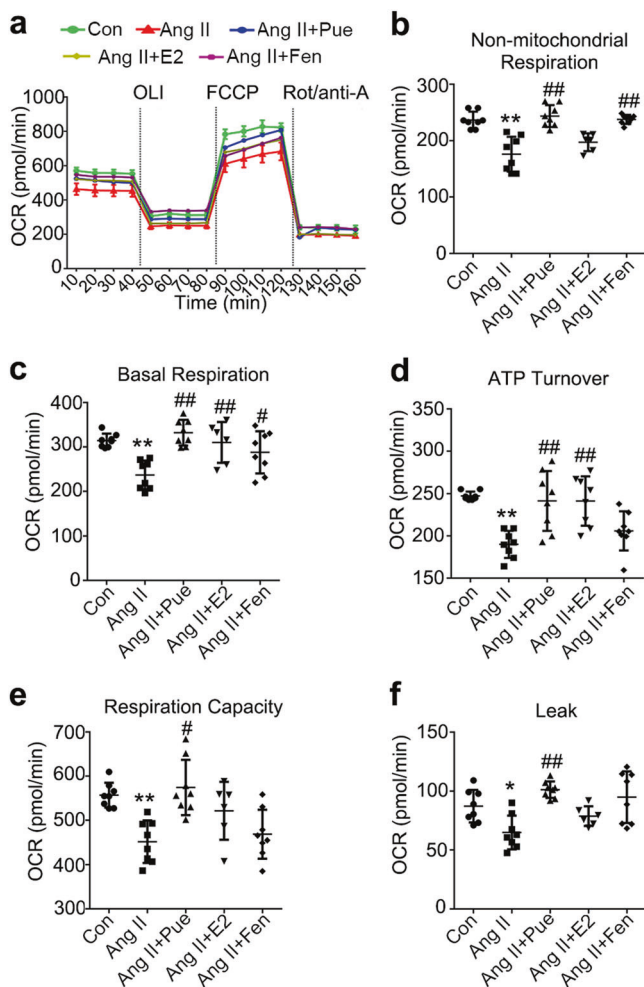
Fig. 8 Puerarin improves mitochondrial function in Ang II-treated cardiomyocytes. **a** Real-time analysis of the oxygen consumption rate (OCR) was performed in response to oligomycin A (OLI, 2 μM), followed by carbonylcyanide p-trifluoromethoxyphenylhydrazone (FCCP, 1 μM) and rotenone/antimycin A (Rot/ant-A; 0.5 μM) in cardiomyocytes subjected to different treatments, as indicated. Representative graph from two independent experiments ($n = 4$ wells/group/experiment). **b–f** Nonmitochondrial respiration (b), basal respiration (c), ATP turnover (d), respiration capacity (e), and leakage (f) in NRCMs under different treatments. Data are presented as the mean ± SD. Statistical significance was determined using one-way ANOVA coupled with Tukey's multiple comparison post hoc test. $^*P < 0.05$ vs. Con group; $^\#P < 0.05$ vs. Ang II group; data are representative of two independent experiments

therapy may increase the risk of breast cancer [1]. Puerarin, a phytoestrogen, demonstrated significantly lower activity than E2 in enhancing the proliferation of MCF-7 cells [31]. In the present study, puerarin prevented cardiac hypertrophy and fibrosis in AAC-treated OVX rats and inhibited the increase in the BW of rats. Its effects are similar to those observed with E2.

PPARs play a central role in regulating the combustion and storage of dietary lipids, essentially acting as sensors for fatty acids and their metabolic intermediates. Cardiac metabolism is transcriptionally regulated by the PPAR family. The expression of PPARα is high in tissues with an elevated capacity for fatty acid oxidation, such as the heart. Activation of PPARα by a ligand triggers its conformational changes and recruits a

coactivator to the promoter regions of target genes (e.g., genes encoding key enzymes in fatty acid metabolism) to initiate transcription [32, 33]. It was previously reported that the absence of PPARα resulted in a more pronounced hypertrophic growth response and cardiac dysfunction in mice under pressure overload [29]. Similarly, PGC-1α protected cardiomyocytes from hypertrophy [34], while PGC-1β deficiency accelerated the transition to heart failure in mice with pressure-overload hypertrophy [35]. In the liver of ovariectomized rats, the mRNA levels of PPARα and PGC-1α were obviously lower than those reported in sham-operated rats [36, 37]. However, the role of the PPARα/PGC-1 pathway in estrogen deficiency-induced myocardial dysfunction remains unknown. Our results showed that the expression of PPARα, PGC-1α, and PGC-1β was decreased in rats with hypertrophic myocardia induced by AAC and OVX. However, the expression of PPARγ did not demonstrate a significant change. In the myocardium, activation of PPARα induced the expression of genes encoding the cellular fatty acid utilization pathway [38, 39]. Our results revealed that in the hearts of AAC-treated OVX rats, the expression of genes involved in fatty acid β-oxidation (i.e., *Cpt1a*, *Cpt1b*, and *Lcad*) was significantly decreased. Similar changes were observed in NRCMs treated with Ang II. These data indicated that the PPARα/PGC-1 pathway was deficient in AAC- and OVX-induced cardiac hypertrophy. Further experiments revealed that, similar to E2 and fenofibrate, puerarin upregulated the expression of PPARα, PGC-1α, and PGC-1β. Simultaneously, puerarin increased the mRNA levels of *Cpt1a*, *Cpt1b*, and *Lcad* in the hearts of AAC-treated OVX rats and Ang II-treated cardiomyocytes. However, E2 only upregulated the expression of *Lcad*. Moreover, puerarin also decreased the fatty acid content and increased the ATP content in NRCMs. These data indicated that puerarin promoted the metabolism of fatty acids, and its effect on improving fatty acid utilization was better than that observed with E2.

The PPARα/PGC-1 pathway regulates the capacity for fatty acid uptake and oxidation, and it is required for mitochondrial biogenesis. PGC-1α is a pivotal molecular link between cellular FA metabolism and the mitochondrial biogenic program. The ERR family (ERRα, ERRβ, and ERRγ) of orphan nuclear receptors is an important cardiac target of PGC-1α that drives the increased expression of genes encoding fatty acid β-oxidation and oxidative phosphorylation enzymes [40]. NRF-1 is a nuclear-encoded transcription factor that is co-activated by PGC-1α to regulate the transcription of genes involved in mitochondrial oxidative phosphorylation, mtDNA transcription and replication, and mitochondrial biogenesis [41]. NRF1 subsequently regulates downstream genes, including TFAM, to maintain mtDNA replication and transcription [42]. In our study, ERRα, NRF1, and TFAM proteins were detected in the hearts of rats from each group, as well as in NRCMs. Eight weeks after AAC and OVX, treatment with puerarin significantly increased the protein levels of ERRα, NRF1, and TFAM in the cardiac tissues of rats. In NRCMs treated with Ang II, the protein levels of ERRα, NRF1, and TFAM were also upregulated by puerarin. We further detected the ΔΨm in NRCMs. In NRCMs treated with Ang II, the dissipation of ΔΨm was reversed by puerarin. We also assessed mitochondrial function in NRCMs through a mitochondrial stress test. The key parameters of mitochondrial respiration were examined by consecutively exposing cardiomyocytes to oligomycin, FCCP, rotenone, and antimycin A. Oligomycin inhibited ATP synthase and reduced the OCR. FCCP uncoupled oxygen consumption from ATP production and increased the OCR to a maximal value. Antimycin A and rotenone targeted the electron transport chain and reduced the OCR to a minimal value. In NRCMs treated with Ang II, the decreased basal respiration, ATP-linked respiration, proton leakage, maximal

Puerarin prevents cardiac hypertrophy via PPARα in OVX rats
N Hou et al.

65
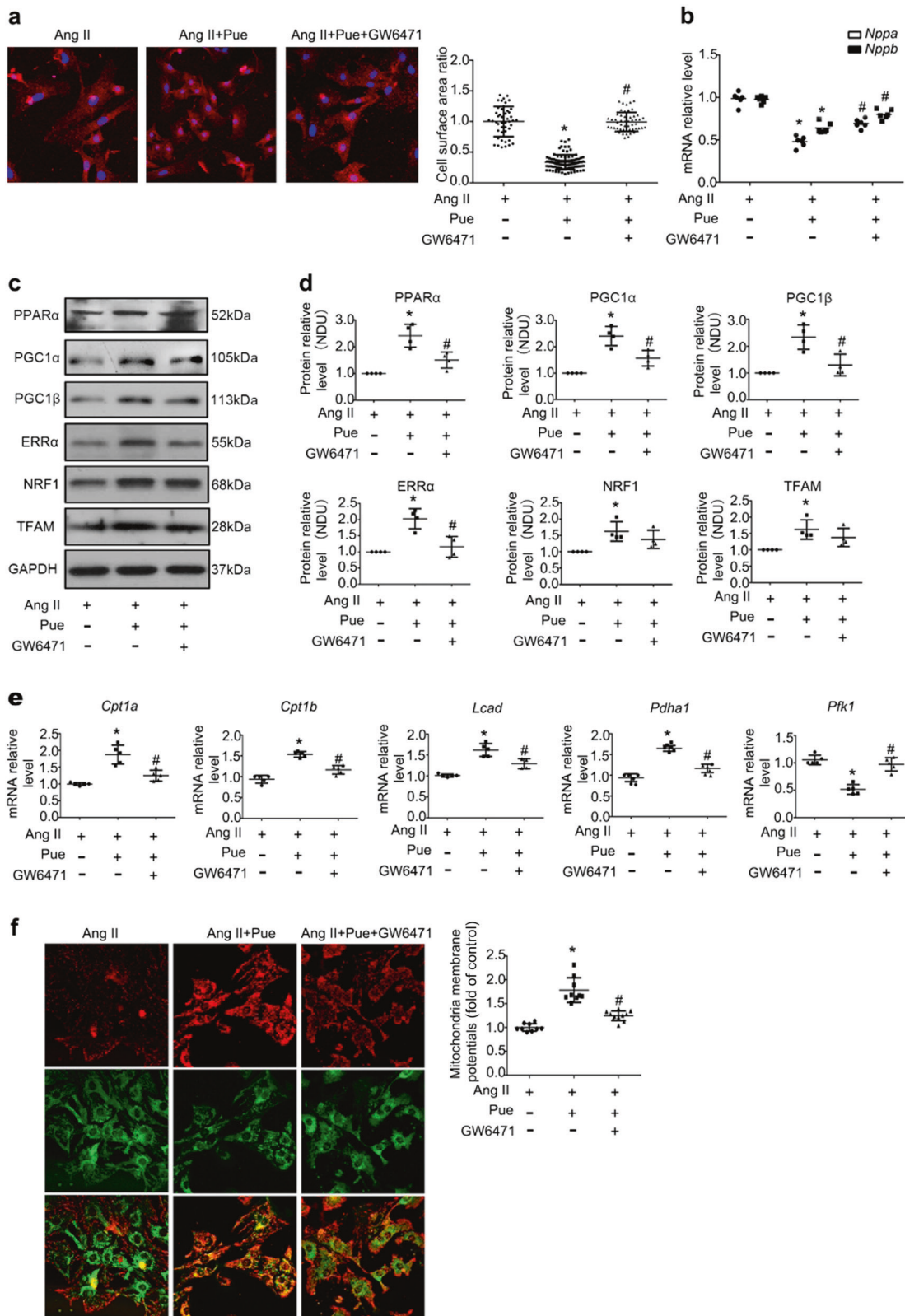
respiration capacity, and nonmitochondrial respiration OCR were obviously increased after treatment with puerarin. In addition, GW6471 partially blocked the beneficial effects of puerarin on NRCMs.

In conclusion, puerarin can prevent cardiac hypertrophy by regulating energy metabolism remodeling via activation of the PPARα/PGC-1 pathway in estrogen deficiency-induced myocardial dysfunction. These findings may provide a pharmacological

Puerarin prevents cardiac hypertrophy via PPARα in OVX rats
N Hou et al.

66

Fig. 9 Puerarin protects against cardiomyocyte hypertrophy through activation of PPARα. **a**: Representative confocal images and measurement of surface area of cardiomyocytes subjected to different treatments, as indicated; $n = 40–50$ cells per group. **b** Reverse transcription-polymerase chain reaction analysis of *Nppa* and *Nppb* in NRCMs subjected to the indicated treatments. Data are representative of five independent experiments. **c, d** Representative Western blots of whole lysates (**c**) and fold changes (**d**) in the relative densitometric values of PPARα, PGC-1α, PGC-1β, ERRα, NRF1, and TFAM in NRCMs under different treatments. Data are representative of four independent experiments. **e** Reverse transcription-polymerase chain reaction analysis of *Cpt1a*, *Cpt1b*, *Lcad*, *Pdha1*, and *Pfk1* in treated NRCMs. Data are representative of six independent experiments. **f** Representative confocal images of JC-1 staining and quantitative analysis of fluorescence in treated NRCMs. Scale bar = 50 μm. Data are presented as the mean ± SD. Statistical significance was determined using one-way ANOVA coupled with Tukey's multiple comparison post hoc test. $^{*}P < 0.05$ vs. Con group; $^{\#}P < 0.05$ vs. Ang II group; $n = 10–12$ cells per group

Table 3. Content of ATP and NEFA in Ang II and puerarin cotreated NRCMs without or with incubation with GW6471

	Ang II	AngII+Pue	Ang II + Pue+GW6471
ATP (μmol·mg^{-1})	101.65 ± 22.40	241.16 ± 30.60*	150.93 ± 22.84$^{\#}$
NEFA (mmol·mg^{-1})	0.54 ± 0.13	0.27 ± 0.10*	0.35 ± 0.05

Data are presented as the mean ± SD. Statistical significance was determined using one-way ANOVA coupled with Tukey's multiple comparison post hoc test. $^{*}P < 0.05$ vs. Ang II group; $^{\#}P < 0.05$ vs. Ang II + Pue group. Data are representative of six independent experiments
ATP adenosine triphosphate, *NEFA* non-esterified fatty acid, *NRCMs* neonatal rat cardiomyocytes

approach to prevent the development of heart failure in postmenopausal women.

AUTHOR CONTRIBUTIONS
Participated in research design: NH, YH, SAC, WCY, CFL, and MSC. Conducted experiments: NH, YH, SAC, WCY, XWL, AQL, CFC, LRL, and GJZ. Supervised experiments: CFL and MSC. Performed data analysis: YH, NH, SAC, WCY, and LRL. Contributed new reagents or analytic tools: XXQ, DFC, JXX, SML, and XHC. Wrote or contributed to the writing of the manuscript: NH, YH, and CFL.

ADDITIONAL INFORMATION

REFERENCES
1. Collins P, Rosano G, Casey C, Daly C, Gambacciani M, Hadji P, et al. Management of cardiovascular risk in the peri-menopausal woman: a consensus statement of European cardiologists and gynaecologists. Eur Heart J. 2007;28:2028–40.
2. Bhuiyan MS, Shioda N, Fukunaga K. Ovariectomy augments pressure overload-induced hypertrophy associated with changes in Akt and nitric oxide synthase signaling pathways in female rats. Am J Physiol Endocrinol Metab. 2007;293:E1606–14.
3. Boardman H, Hartley L, Eisinga A, Main C, Figuls MR. Cochrane corner: oral hormone therapy and cardiovascular outcomes in post-menopausal women. Heart. 2016;102:9–11.
4. Kamo T, Akazawa H, Komuro I. Cardiac nonmyocytes in the hub of cardiac hypertrophy. Circ Res. 2015;117:89–98.
5. Allard MF. Energy substrate metabolism in cardiac hypertrophy. Curr Hypertens Rep. 2004;6:430–5.
6. Oka T, Akazawa H, Naito AT, Komuro I. Angiogenesis and cardiac hypertrophy: maintenance of cardiac function and causative roles in heart failure. Circ Res. 2014;114:565–71.
7. Taegtmeyer H, Golfman L, Sharma S, Razeghi P, van Arsdall M. Linking gene expression to function: metabolic flexibility in the normal and diseased heart. Ann N Y Acad Sci. 2004;1015:202–13.
8. Lehman JJ, Kelly DP. Gene regulatory mechanisms governing energy metabolism during cardiac hypertrophic growth. Heart Fail Rev. 2002;7:175–85.
9. Kolwicz SC Jr, Tian R. Glucose metabolism and cardiac hypertrophy. Cardiovasc Res. 2011;90:194–201.
10. Goldberg IJ, Trent CM, Schulze PC. Lipid metabolism and toxicity in the heart. Cell Metab. 2012;15:805–12.
11. Planavila A, Calvo RR, Vazquez-Carrera M. Peroxisome proliferator-activated receptors and the control of fatty acid oxidation in cardiac hypertrophy. Mini-Rev Med Chem. 2006;6:357–63.
12. Young ME, Laws FA, Goodwin GW, Taegtmeyer H. Reactivation of peroxisome proliferator-activated receptor alpha is associated with contractile dysfunction in hypertrophied rat heart. J Biol Chem. 2001;276:44390–5.
13. Schilling J, Kelly DP. The PGC-1 cascade as a therapeutic target for heart failure. J Mol Cell Cardiol. 2011;51:578–83.
14. Zhou YX, Zhang H, Peng C. Puerarin: a review of pharmacological effects. Phytother Res. 2014;28:961–75.
15. Song XP, Chen PP, Chai XS. Effects of puerarin on blood pressure and plasma renin activity in spontaneously hypertensive rats. Acta Pharmacol Sin. 1988;9:55–8.
16. Gao L, Ji X, Song J, Liu P, Yan F, Gong W, et al. Puerarin protects against ischemic brain injury in a rat model of transient focal ischemia. Neurol Res. 2009;31:402–6.
17. Zhang S, Chen S, Shen Y, Yang D, Liu X, Sun-Chi AC, et al. Puerarin induces angiogenesis in myocardium of rat with myocardial infarction. Biol Pharmacol Bull. 2006;29:945–50.
18. Hsu FL, Liu IM, Kuo DH, Chen WC, Su HC, Cheng JT. Antihyperglycemic effect of puerarin in streptozotocin-induced diabetic rats. J Nat Prod. 2003;66:788–92.
19. Yan LP, Chan SW, Chan ASC, Chen SL, Ma XJ, Xu HX. Puerarin decreases serum total cholesterol and enhances thoracic aorta endothelial nitric oxide synthase expression in diet-induced hypercholesterolemic rats. Life Sci. 2006;79:324–30.
20. Yuan Y, Zong J, Zhou H, Bian ZY, Deng W, Dai J, et al. Puerarin attenuates pressure overload-induced cardiac hypertrophy. J Cardiol. 2014;63:73–81.
21. Chen G, Pan SQ, Shen C, Pan SF, Zhang XM, He QY. Puerarin inhibits angiotensin II-induced cardiac hypertrophy via the redox-sensitive ERK1/2, p38 and NF-kappa B pathways. Acta Pharmacol Sin. 2014;35:463–75.
22. Chen G, Cao Q, Cui X, Pan S, Shen C, Liu L. Puerarin suppresses angiotensin II-induced cardiac hypertrophy by inhibiting NADPH oxidase activation and oxidative stress-triggered AP-1 signaling pathways. J Pharm Pharmacol Sci. 2015;18:235–48.
23. Hou N, Cai B, Ou CW, Zhang ZH, Liu XW, Yuan M, et al. Puerarin-7-O-glucuronide, a water-soluble puerarin metabolite, prevents angiotensin II-induced cardiomyocyte hypertrophy by reducing oxidative stress. Naunyn Schmiedebergs Arch Pharmacol. 2017;390:535–45.
24. Liu B, Wu Z, Li Y, Ou C, Huang Z, Zhang J, et al. Puerarin prevents cardiac hypertrophy induced by pressure overload through activation of autophagy. Biochem Biophys Res Commun. 2015;464:908–15.
25. Zhang X, Liu Y, Han Q. Puerarin attenuates cardiac hypertrophy partly through increasing Mir-15b/195 expression and suppressing non-canonical transforming growth factor β (Tgfβ) signal pathway. Med Sci Monit. 2016;22:1516–23.
26. Zhao GJ, Hou N, Cai SA, Liu XW, Li AQ, Cheng CF, et al. Contributions of Nrf2 to puerarin prevention of cardiac hypertrophy and its metabolic enzymes expression in rats. J Pharmacol Exp Ther. 2018;366:458–69.
27. Cai SA, Hou N, Zhao GJ, Liu XW, He YY, Liu HL, et al. Nrf2 is a key regulator on puerarin preventing cardiac fibrosis and upregulating metabolic enzymes UGT1A1 in rats. Front Pharmacol. 2018;9:540.
28. Hou N, Luo MS, Liu SM, Zhang HN, Xiao Q, Sun P, et al. Leptin induces hypertrophy through activating the peroxisome proliferator-activated receptor alpha

Puerarin prevents cardiac hypertrophy via PPARα in OVX rats
N Hou et al.

67

pathway in cultured neonatal rat cardiomyocytes. Clin Exp Pharmacol Physiol. 2010;37:1087–95.

29. Smeets PJ, Teunissen BE, Willemsen PH, van Nieuwenhoven FA, Brouns AE, Janssen BJ, et al. Cardiac hypertrophy is enhanced in PPAR alpha-/- mice in response to chronic pressure overload. Cardiovasc Res. 2008;78:79–89.

30. Al-Safi ZA, Polotsky AJ. Obesity and menopause. Best Pract Res Clin Obstet Gynaecol. 2015;29:548–53.

31. Cherdshewasart W, Traisup V, Picha P. Determination of the estrogenic activity of wild phytoestrogen-rich Pueraria mirifica by MCF-7 proliferation assay. J Reprod Dev. 2008;54:63–7.

32. Finck BN. The PPAR regulatory system in cardiac physiology and disease. Cardiovasc Res. 2007;73:269–77.

33. Yu S, Reddy JK. Transcription coactivators for peroxisome proliferator-activated receptors. Biochim Biophys Acta. 2007;1771:936–51.

34. Liu XP, Gao H, Huang XY, Chen YF, Feng XJ, He YH, et al. Peroxisome proliferator-activated receptor gamma coactivator 1 α protects cardiomyocytes from hypertrophy by suppressing calcineurin-nuclear factor of activated T cells c4 signaling pathway. Transl Res. 2015;166:459–73.

35. Riehle C, Wende AR, Zaha VG, Pires KM, Wayment B, Olsen C, et al. PGC-1β deficiency accelerates the transition to heart failure in pressure overload hypertrophy. Circ Res. 2011;109:783–93.

36. Zheng W, Rogoschin J, Niehoff A, Oden K, Kulling SE, Xie M, et al. Combinatory effects of phytoestrogens and exercise on body fat mass and lipid metabolism in ovariectomized female rats. J Steroid Biochem Mol Biol. 2018;178:73–81.

37. Paquette A, Wang D, Jankowski M, Gutkowska J, Lavoie JM. Effects of ovariectomy on PPAR alpha, SREBP-1c, and SCD-1 gene expression in the rat liver. Menopause. 2008;15:1169–75.

38. Gilde AJ, van der Lee KA, Willemsen PH, Chinetti G, van der Leij FR, van der Vusse GJ, et al. Peroxisome proliferator-activated receptor (PPAR) alpha and PPARbeta/delta, but not PPARgamma, modulate the expression of genes involved in cardiac lipid metabolism. Circ Res. 2003;92:518–24.

39. Barger PM, Brandt JM, Leone TC, Weinheimer CJ, Kelly DP. Deactivation of peroxisome proliferator-activated receptor-alpha during cardiac hypertrophic growth. J Clin Invest. 2000;105:1723–30.

40. Dufour CR, Wilson BJ, Huss JM, Kelly DP, Alaynick WA, Downes M, et al. Genome-wide orchestration of cardiac functions by the orphan nuclear receptors ERRalpha and gamma. Cell Metab. 2007;5:345–56.

41. Wu Z, Puigserver P, Andersson U, Zhang C, Adelmant G, Mootha V, et al. Mechanisms controlling mitochondrial biogenesis and respiration through the thermogenic coactivator PGC-1. Cell. 1999;98:115–24.

42. Huss JM, Kelly DP. Nuclear receptor signaling and cardiac energetics. Circ Res. 2004;95:568–78.